

High-pressure phase transitions of Zn_2SiO_4 : In-situ Raman spectroscopic study

KANZAKI, Masami^{1*}

¹Inst. Study Earth Inst., Okayama U.

Zn and Mg have similar ionic radii, but their crystal chemical behaviors in silicates are quite different. In phase relation of Zn_2SiO_4 system, I (willemitite), II, III, IV, V (modified spinel) phases are known (Syono et al., 1971), but only V has common structure with Mg_2SiO_4 system. Neither olivine nor spinel structures exist in Zn_2SiO_4 . This difference is quite interesting in terms of crystal chemistry. Recently, we have determined crystal structures of phases III and IV, and suggested that these phases are retrograde phases (Liu et al., 2013). In order to check this possibility, first-principles DFT calculations were conducted, and pressure-induced transitions for III and IV were discovered (Kanzaki, JpGU meeting 2014). In the present study, these transitions were checked experimentally using in-situ Raman spectroscopy. Phase II was also studied, since this phase is found to transform to (metastable) spinel structure by first-principles calculations.

For observation of phase transitions, in-situ Raman spectroscopy of samples in diamond anvil cell (DAC) was conducted. Symmetric DAC was used with low-fluorescence diamond (500 micron culet). Samples of phases II, III and IV were fragments made by multi-anvil press quench experiments (Liu et al., 2013). Gasket was made of SUS301H with 250 micron thick, and 200 micron hole after indentation was made. Pressure medium was alcohol mixture for phases III and IV, and KBr for phase II. Pressure was determined by Ruby fluorescence technique. All experiments were done at room temperature.

For phase III, Raman spectrum at 5.5 GPa gradually changed to new spectrum during compression process. During decompression, back transformation was observed at 1.5 GPa, and original spectrum of phase III was observed again. For phase IV, a transition was found at 2.5 GPa for both compression and decompression processes. For phase II, new spectrum appeared at about 13 GPa during compression process, but peaks were broad, possibly due to non-hydrostatic condition. Change of Raman spectrum at each transition was discontinuous, so these transitions should be 1st order in nature.

Present in-situ Raman spectroscopic studies confirmed that phases III and IV are indeed retrograde phases. Observed transition pressures were lower than their supposed stable pressure region, consistent with previous quench experiments (Syono et al., 1971). These results were consistent with our first-principles study too. However, for phase transition of III, octahedral Si is expected for high-pressure phase. Rather low observed transition pressure (5.5 GPa) suggests that the transition is not same as that observed by first-principles calculation.

Currently, structural identification of high-pressure phases is underway by calculation of Raman spectra of candidate phases from first-principles.

Reference:

Liu, X., Kanzaki, M., Xue, X. (2013) Crystal structures of Zn_2SiO_4 III and IV synthesized at 6.5-8 GPa and 1,273 K, *Phys. Chem. Minerals*, **40**, 467-478.

Syono, Y., Akimoto, S., Matsui, M. (1971) High pressure transformations in zinc silicates, *J. Solid State Chem.*, **3**, 369-380.

Keywords: Zn_2SiO_4 , phase transition, Raman spectroscopy, high pressure, crystal chemistry, crystal structure

OH defects in hydrothermally synthesized monazite (LaPO₄) and xenotime (YPO₄) single crystals

ABE, Takeyasu^{1*}; NAKAMURA, Michihiko¹; KURIBAYASHI, Takahiro¹

¹Department of Earth Sciences, Tohoku University

Monazite and xenotime are common REE (rare earth elements: here considered as Y and lanthanoid) minerals in crustal metamorphic and granitic rocks (e.g. Spear and Pyle 2002). These minerals are widely used in petrologic studies as a U-Th-Pb geochronometer (e.g. Parrish 1990, Suzuki et al. 1991) and a geothermometer (e.g. Gratz and Heinrich 1997, Pyle et al. 2001 and Viskupic and Hodges 2001). Furthermore, these minerals have been focused on as a functional material owing to their several exceptional physical and chemical properties such as the high fusion temperature, high chemical durability and wide stability fields, etc. (see also reviewed papers: e.g. Boatner 2002, Kolitsch and Holstam 2004, Clavier et al. 2011).

The X-ray analyses for these minerals has been conducted by Ni et al. (1995). Monazite has monoclinic symmetry with space group $P2_1/n$, and preferentially incorporates LREE (light rare earth elements, here La~Gd). On the other hand, xenotime has tetragonal symmetry with space group $I4_1/amd$ (isostructure with zircon), and preferentially incorporates HREE (heavy rare earth elements, here Tb~Lu + Y). Monazite and xenotime can contain trace amount of hydrogen as nominally anhydrous minerals (NAMs). However, only few studies have been reported on infrared spectroscopic measurements of monazite and xenotime. In this study, we conducted polarized infrared spectroscopic observation on hydrothermally synthesized monazite (LaPO₄) and xenotime (YPO₄) single crystals.

The single crystals of monazite and xenotime, synthesized with a piston-cylinder apparatus under a pressure of 1.0 GPa and cut perpendicular and parallel to the elongated direction, are mounted and doubly polished (i.e., monazite: E is nearly perpendicular to Y or Z , xenotime: $E \perp c$ or a). The polarized infrared spectra of monazite and xenotime single crystals were measured in the transmission mode by Nicolet iN10 (Thermo Scientific Inc.).

Monazite crystals show two pleochroic absorption bands at 3164 cm⁻¹ (FWHM = ca. 50 cm⁻¹) and around 3330 cm⁻¹ (FWHM = ca. 140 cm⁻¹). On the other hand, xenotime crystals show a pleochroic absorption band at 3302 cm⁻¹ (FWHM = ca. 10 cm⁻¹). According to obtained absorption figures, the OH dipole in monazite is weakly oriented to [110], while in xenotime, it is strongly oriented perpendicular to c -axis. Based on these results, we suggest the OH incorporation models as shown in Figure 1. Two incorporation models must be considered on monazite due to the n glide symmetric element. The charge balancing mechanism in monazite is expressed as $REE^{3+} \leftrightarrow \square_{REE} + 3H^+$. In contrast, the charge balance in xenotime is maintained by the reaction of $REE^{3+} + O^{2-} \leftrightarrow \square_{REE} + \square_O + H^+$. When the Libowitzky (1999) correlation is applied to the obtained band positions (monazite: 3164 cm⁻¹ and 3330 cm⁻¹, xenotime: 3302 cm⁻¹), the O-O distance of 2.69, 2.76 and 2.74 Å is estimated, respectively. Considering the estimated inter-atomic distance and our OH incorporation models, we could suggest the formation of vacant REE site cause the slight deformation of monazite and xenotime crystal lattices.

Keywords: Monazite, Xenotime, Hydrothermal syntheses, Nominally Anhydrous Minerals, Polarized infrared spectroscopy

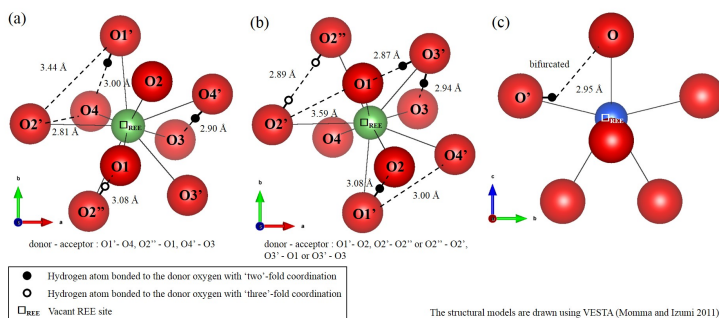


Figure 1. OH incorporation models of monazite (a), (b) and xenotime (c). (a), (b) Two types of hydrogen sites, which corresponding to the coordination number of the donor oxygen, are considered. The two band positions at 3164 cm⁻¹ and 3330 cm⁻¹ would be brought by the coordination number difference of the donor oxygen. (c) The hydrogen position would demand a bifurcated hydrogen bonding. This incorporation model is also proposed by Talla et al. (2011). Additionally in zircon (isostructural with xenotime), the same incorporation model is proposed by Nasdala et al. (2001).

The site and coordination number of oxygen atom in monazite and xenotime can be summarized as below. The oxygen atom in monazite occupies the four general positions (from O1 to O4). O1, O3 and O4 bond with two REE atoms and one P atom. Only O2 bonds with three REE atoms and one P atom. On the other hand, the oxygen atom in xenotime has only one site placed in a mirror plane, and bonds with two REE atoms and one P atom. For more details, see also Ni et al. (1995).

X-ray and neutron diffraction experiments on hydrous silica glass under pressure

URAKAWA, Satoru^{1*} ; INOUE, Toru² ; HATTORI, Takanori³ ; SANO, Asami³ ; KIKEGAWA, Takumi⁴ ;
FUNAKOSHI, Ken-ichi⁵ ; MIBE, Kenji⁶ ; KOHARA, Shinji⁷

¹Dept Earth Sci, Okayama Univ, ²GRC, Ehime Univ, ³J-PARC, JAEA, ⁴PF, KEK, ⁵CROSS, ⁶ERI, Univ Tokyo, ⁷JASRI

We have studied structure of hydrous silica glass by using X-ray and Neutron diffraction experiments up to 10 GPa at ambient temperature. Hydrous silica glass was synthesized by quenching from melts under pressure, which contains 13 wt % of D₂O. X-ray diffraction experiments were conducted at BL04B2 of SPring-8 and AR-NE5 of Photon Factory. Neutron diffraction experiments were carried out at BL11 of MLF, J-PARC. Both X-ray and neutron diffractions show the shift of the FSDP of structure factor toward higher Q with increasing pressure, indicating the shrinkage of the intermediate range order with pressure. The radial distribution functions shows that the SiO₄ unit does not change up to 10 GPa but the Si-Si distance decrease with pressure. These also indicate the change of the intermediate range order. D-O distance in the hydrous silica glass is nearly constant, 0.92 Å. The changes of silica framework with pressure in hydrous silica glass are similar to those in dry silica glass.

Keywords: silicate glass, magma, neutron

Structural change of hauyne with increasing temperature

AOKI, Satoshi^{1*} ; KURIBAYASHI, Takahiro¹ ; NAGASE, Toshiro²

¹Graduate school of science, Tohoku University, ²The Tohoku University Museum, Tohoku University

Hauyne, $\text{Na}_3\text{CaSi}_3\text{Al}_3\text{O}_{12}\text{SO}_4$, belongs to the sodalite group. Most of nature hauynes have modulated structure. Previous researchers (e.g. Saalfeld, 1961; Tsuchiya and Takeuchi, 1985) studied the modulated structure of hauynes from some localities by X-ray and electron diffraction methods. The results from heating experiments showed there is a discontinuity of thermal expansion between 550 °C and 700 °C, and the thermal expansion coefficient of hauyne changed to small value above 700 °C (e.g. Taylor, 1968). Disappearance of satellite reflections, which indicated the phase transition, was observed between 390 °C and 407 °C by high temperature in situ synchrotron X-ray powder diffraction experiment (Hassan *et al.*, 2004). The relationship between the structural change and the discontinuity of thermal expansion is unclear. High temperature in situ single crystal X-ray diffraction experiments were conducted to investigate relationship between structural change and discontinuity of thermal expansion.

Hauyne from eifel, German was used to our experiments. The backscattered electron images showed the chemical composition of the crystal was homogeneous, and its chemical formula was determined as $\text{Na}_{2.83}\text{Ca}_{0.95}\text{K}_{0.21}\text{Si}_{3.06}\text{Al}_{2.93}\text{O}_{12}(\text{SO}_4)_{0.95}\text{Cl}_{0.03}$ by using an energy dispersive X-ray spectrometer (JEOL, JSM-7001F). High temperature in situ single crystal X-ray diffraction experiments were examined by using an imaging plate type X-ray diffractometer (Rigaku, R-Axis IV++) with a horseshoe-shaped Pt heater (Huber). Observation of the satellite peaks and determination of cell parameter were performed at eight points between 20 °C and 700 °C. Crystal Clear-SM 1.4.0 (Rigaku) was used for data analysis.

The lattice parameter of the modulated structure of the sample was approximately eight times long as the basic structure. Satellite reflections were disappeared around 700 °C although they were observed until 600 °C, therefore, structural change was indicated in the temperature range. Also, the axial length of a-axis increased monotonously with increasing temperature, and the thermal expansion coefficient between 600 °C and 700 °C have smaller value. The results suggested structural change of hauyne would affect the discontinuity of thermal expansion.

Keywords: hauyne, modulated structure, single-crystal X-ray diffraction, high temperature, in situ observation

Application of free volume theory to the model of thermal pressure for NaCl

SUMITA, Tatsuya^{1*}

¹Geological Survey of Japan, National Institute of Advanced Industrial Science and Technology (AIST)

Mie-Gruneisen type equation is frequently used for the Temperature-Pressure-Volume equation of state (EoS) for pressure standard materials and minerals in the Earth's interior. Mie-Gruneisen type equation consists of the isothermal compression term and the thermal pressure term. In the thermal pressure term, Gruneisen parameter (γ) is very important thermodynamic parameter. It is known that γ relates to the property of isothermal compression as Slater's equation [1]. From the studies of molecular dynamics and potential theory, Barton and Stacey [2] advanced the free volume theory [3], and then derived the equation (called as "modified free volume formula" or "Barton-Stacey formula"), which can calculate practical γ values from the parameters of an isothermal compression curve. It is important that this formula gives theoretically support for volume dependence of γ , and moreover reduces the parameters of total EoS in number.

In this study, we apply Barton-Stacey formula to NaCl-B1 phase. We use the CT-EoS data as experimental reference, and the thermal pressure model, which include effect of intrinsic anharmonicity, as base model [4]. The power law γ at zero temperature in the base model is replaced by Barton-Stacey formula with the parameters of the isothermal EoS at zero temperature [5,6]. The value of f , which is the parameter relating to the randomness of thermal motion of atoms in Barton-Stacey formula, is estimated from using the free volume γ [3]. The present model reproduce successfully values of γ and specific heats without sacrificing accuracy, in spite of reducing one parameter of the EoS.

References

- [1] J.C. Slater: Introduction to Chemical Physics, McGraw-Hill, New York (1939)
- [2] M.A. Barton, F.D. Stacey: Phys. Earth Planet. Int., 39, 167 (1985)
- [3] V.Ya. Vashchenko, V.N. Zubarev: Sov. Phys. Solid State, 5, 653 (1963)
- [4] T. Sumita, A. Yoneda: Phys. Chem. Minerals, 41, 91 (2014)
- [5] T. Sumita: Special Issue of Rev. High Pressure Sci. Tech., 24, 143 (2014) in Japanese
- [6] A. Keane: Australian J. Phys., 7, 323 (1954)

Keywords: equation of state, thermal pressure, free volume theory, Gruneisen parameter, thermodynamics, NaCl-B1 phase

Pressure measurements using diamond and cubic boron nitride

ONO, Shigeaki^{1*}

¹JAMSTEC

Experiments using diamond anvil cells have been important in many studies of crystals and liquids at high pressure and temperature because these cells permit not only optical observation of the sample but also in situ measurement of the sample's physical and chemical properties. The pressure in the sample chamber of such cells is often determined by the shift in the wavenumber of a fluorescence line of ruby inside the sample chamber. However, the intensity of the ruby fluorescence decreases rapidly with increasing temperature. It is known that the first-order Raman mode of diamond anvil has been considered as a strong candidate of pressure marker because its Raman signal is intense and the diamond is always used as the anvil material in the DAC experiments. Cubic boron nitride (*c*-BN) is also a candidate of pressure marker because of chemical inertness and high temperature stability. It is the purpose of this study to present the dependences of pressure and temperature in the Raman lines of diamond and *c*-BN, using techniques combining synchrotron X-ray diffraction measurement with the Raman spectroscopic measurement.

The first-order Raman line at the culet face of the diamond anvil was investigated because the high-frequency edge of the Raman mode was correlated with the normal stress at the culet face of the diamond anvil. Thus, the edge frequency is a function of pressure and temperature in the sample chamber of the DAC experiment. Raman spectrum of *c*-BN exhibits two intense lines at 1054 and 1305 cm^{-1} under ambient conditions, corresponding to the Brillouin zone center transverse optical (*TO*) and longitudinal optical (*LO*) modes, respectively. The Raman line of the *LO* mode overlaps an intense Raman line of diamond at pressures higher than 3 GPa. Therefore, it is difficult to observe the *LO* line in high-pressure experiments using the diamond anvil cell. In contrast, the *TO* mode could be used as the pressure calibrant in diamond anvil cells under high pressure and temperature conditions.

High-pressure X-ray diffraction experiments were carried out in an external heated diamond anvil cell. The small sample sandwiched between pellets of NaCl powder was loaded into a hole that had predrilled into a rhenium gasket. The heating temperature was up to 1000 K, and was recorded using the *K*-type of thermocouples. The sample was probed using angle-dispersive X-ray diffraction, located on the synchrotron beam line, at BL10XU of the Spring-8. The angle-dispersive X-ray diffraction patterns were obtained on the X-ray CCD collection system. The pressure was calculated from the MgO unit cell volume using the equation of state (EOS) for MgO.

Experimental runs were carried out at pressures of up to 110 GPa. In each run, the sample was compressed to the desired pressure, and then heated to measure the shift of the Raman spectra of diamond [1] and *c*-BN [2] at high pressure and temperature. At each pressure increment, the cell was screwed to hold the sample pressure and the Raman spectra were acquired at 300-1000 K with decreasing temperature. Two peaks, which corresponded to the *TO* mode of *c*-BN and the *LTO* mode of diamond, were identified at high pressures and temperatures. At pressures higher than 90 GPa, the *TO* mode of *c*-BN overlapped with the intense Raman peak of diamond. This indicated that *c*-BN can be used as the pressure calibrant at pressures below 90 GPa in diamond anvil cell experiments [2].

[1] Ono et al., Raman spectra of culet face of diamond anvils and application as optical pressure sensor to high temperatures, *J. Appl. Phys.*, 116, 053517 (2014).

[2] Ono et al., *In situ* Raman spectroscopy of cubic boron nitride to 90 GPa and 800 K, *J. Phys. Chem. Solid*, 76, 120-124 (2014).

Keywords: Diamond, Cubic boron nitride, High pressure and high temperature

Diamond formation from magnesite in the presence of C-H-O fluid under high pressure and temperature

OHFUJI, Hiroaki^{1*}; IKAWA, Syunta¹; KIMURA, Tomoaki¹

¹Geodynamics Research Center, Ehime University

Diamond formation in the Earth's mantle is believed to be a metasomatic process by fluid/melt with peridotitic and/or eclogitic rocks (e.g. Shirey et al., 2013). The ubiquitous occurrence of nano- to micro fluid inclusions in natural diamond and the result of recent experimental studies (e.g. Sokol et al., 2009) suggest that the presence of C-H-O fluid, which consist of a mixture of H₂O, CO₂, CH₄, etc. plays an important role in diamond forming reaction. The composition of C-H-O fluid depends largely on the surrounding oxygen fugacity. Taking into an account the oxygen fugacity values estimated from diamond-bearing xenoliths, the most major components of such fluids at the depth of 150-200 km are likely H₂O and CH₄ (Shirey et al., 2013). In the deeper mantle, the relative proportion of CH₄ is expected to increase with depth (Frost and McCammon, 2008). In the present work, we studied the diamond formation through the reaction between magnesite and reduced C-H-O fluid at high pressure and high temperature.

A series of high-pressure and high-temperature experiments (up to 30 GPa, 2000K) were performed by using laser-heated diamond anvil cell (LH-DAC). A small fragment of natural pure magnesite (either polycrystalline aggregate or single crystal) is loaded together with stearic acid (C₁₈H₃₆O₂) or pure CH₄ in a sample chamber drilled in a pre-indented rhenium gasket. Upon laser-heating, the stearic acid is expected to produce CH₄-rich fluid as a result of decomposition reaction (C₁₈H₃₆O₂ → 8CH₄ + 2H₂O + 10C). A dual-beam CO₂ laser system (at Ehime Univ.) or a dual-beam fiber laser system (at SPring-8) was used for the heating. In-situ XRD observation at high pressure and high temperature was conducted in BL10XU of SPring-8. The samples after recovery were examined by XRD, Raman spectroscopy and scanning and transmission electron microscopies.

In-situ XRD observation showed that magnesite, MgCO₃ decomposes into periclase, MgO, brucite, Mg(OH)₂ and diamond in the presence of CH₄-rich fluid at pressures above 18 GPa and at ~2000K. Brucite is likely to be a metastable product, because the formation is usually observed at the beginning of the reaction and its relative proportion decreases with time by being taken over by the formation of periclase. The formation of nanocrystalline diamond was also observed in the samples recovered from the experiments. Although diamond was produced by the decomposition reaction of stearic acid through the equation described above, the reduction of magnesite by CH₄-rich fluid must also have resulted in diamond formation. Inclusion studies of super-deep (lower-mantle derived) diamonds reported that the most dominant mineral phase found in such diamonds is periclase (up to 60%). However, this is not consistent with the result of high-pressure experimental studies using pyrolytic composition, where Mg-perovskite (bridgmanite) is the most dominant. Our result implies that some of the periclase inclusions solely found in those diamonds might have formed as a result of the reaction of Mg-rich carbonate with reduced C-H-O fluid. This means that the information obtained from diamond inclusion does not necessarily reflect the bulk composition of the lower mantle. Furthermore, the formation of periclase at shallower condition (at 18 GPa) suggests that such formed periclase inclusions in diamond may not be used as indicator of lower-mantle origin.

Keywords: Diamond, Magnesite, C-H-O fluid, High pressure and high temperature

High-pressure behavior of cuprospinel CuFe_2O_4 : the Jahn-Teller effect of Cu^{2+} on the spinel structure

KYONO, Atsushi^{1*}; NAKAMOTO, Yuki²; KATO, Masato¹

¹Graduate School of Life and Environmental Sciences, University of Tsukuba, ²Center for Science and Technology under Extreme Conditions, Osaka University

The Jahn-Teller-effect at Cu^{2+} in cuprospinel CuFe_2O_4 was investigated using high-pressure single-crystal synchrotron x-ray diffraction (XRD) techniques at beamline BL10A at the Photon Factory, KEK, Japan. Six data sets were collected in the pressure range from ambient to 5.9 GPa at room temperature. Structural refinements based on the data were performed at 0.0, 1.8, 2.7, and 4.6 GPa. The unit cell volume of cuprospinel decreases continuously from 590.8 (6) \AA^3 to 579.5 (8) \AA^3 up to 3.8 GPa. Least-squares fitting to a third-order Birch-Murnaghan equation of state yields zero-pressure volume $V_0 = 590.7$ (1) \AA^3 and bulk modulus $K_0 = 188.1$ (4.4) GPa with K' fixed at 4.0. The crystal chemical composition determined by electron-probe analysis and site-occupancy refinement is represented as $^{[4]}[\text{Fe}_{0.901}\text{Cu}_{0.099}]^{[6]}[\text{Fe}_{1.500}\text{Cu}_{0.500}]\text{O}_4$. Most of the Cu^{2+} are preferentially distributed onto the octahedral (M) site of the spinel structure. At 4.6 GPa, a cubic-tetragonal phase transition is indicated by a splitting of the a axis of the cubic structure into a smaller a axis and a longer c axis, with unit cell parameters $a = 5.882$ (1) \AA and $c = 8.337$ (1) \AA . The tetragonal crystal structure with space group $I4_1/amd$ was refined to $R1 = 0.0332$ and $wR2 = 0.0703$ using observed 39 x-ray reflections. The M -O bond distances along the c -axis direction of the unit cell are elongated, whereas those parallel to the a - b plane are compressed. At the T site, on the other hand, the tetrahedral O- T -O bond angles along the c -axis direction of the unit cell increases from 109.47° to 111.7 (6)°, which generates a compressed tetrahedral geometry along the c -axis. The cubic-to-tetragonal transition induced by the Jahn-Teller effect at Cu^{2+} is attributable to the elongation at the M site. The Jahn-Teller distortion by the Cu 3d orbital at the M site is confirmed by *ab-initio* quantum chemical calculations. With the competing distortions between the elongated octahedron and the compressed tetrahedron along the c -axis, the a unit cell parameter is shortened with respect to the c unit cell parameter, giving a c/a ratio slightly greater than unity as referred to cubic lattice ($c/a = 1.002$). The c/a value increases to 1.007 with pressure, suggesting a further variation of the elongated octahedron and the compressed tetrahedron. The variation of c/a ratio of the cuprospinel is similar to that observed in the tetragonally distorted cuprospinel with Cu^{2+} fully occupying the octahedral site of the structure.

Keywords: cuprospinel CuFe_2O_4 , high-pressure, single-crystal synchrotron x-ray diffraction method, Jahn-Teller effect

Crystal growth textures developed in rapid cooling of olivine fine particles

TOKUNAGA, Shinya¹ ; ISOBE, Hiroshi^{2*}

¹Fac. Sci., Kumamoto Univ., ²Grad. Sch. Sci. Tech., Kumamoto Univ.

Olivine is one of the most common mineral in the solid Earth and chondritic meteorites. Olivine crystals show characteristic textures in chondrules depending on heating and cooling histories in chondrule formation processes at the early solar system. In this study, quick heating and cooling experiments of mixed olivine particles were carried out with a fine particles free falling apparatus with controlled gas flow (Isobe and Gondo, 2013). In the run products, characteristic melting and crystal growth textures controlled by phase relations, diffusion, and nucleation and growth behavior of olivine can be seen depending on maximum temperatures and cooling rates.

Starting material is mixed powder of natural olivine (Fo90), fayalite and an artificial olivine (Fo57). The typical diameter of the starting material particles is approximately 100 micron meters. Each particle is single crystal of olivine or mixture of two or three kinds of raw materials. Heating and cooling experiments are carried out in a high temperature furnace with mass flow controllers to regulate oxygen fugacity and total gas flow rate. Oxygen fugacity is controlled to average of FMQ and IW buffer curves in log unit. In the each run, maximum temperature of particles is just above 1500 degree C or 1400 degree C. Gas flow rates are 2.6, 1.3 or 0.65 l/min@RT. Particles can be heated to the maximum temperature within two seconds, are kept approximately one second and quenched within a second. Maximum temperature has negative correlation to diameter of the particles, and cooling rate has positive correlation to the diameter depending on the falling velocity of the particles. Run products show spherical shape when the particles mostly melted, and are crystal fragments when the particles did not melt. The outside shape of the retrieved run products are observed with a scanning electron microscope. Inner textures of the particles are observed on polished section of the particles. Chemical compositions are also analyzed on the sections.

Fayalite grains are completely melted and Fo90 olivine grains are not melted by themselves concordantly with the phase relation of olivine. Internal textures of Fo57 olivine crystals show quick partial melting when the temperature reach solidus temperature. Then, compositional ranges of quench crystals developed in fractional crystallization show negative correlation to cooling rates. Growth rate of quench growth olivine may be much higher than homogenization in heterogeneous silicate melt.

In the mixed olivine particles, relict crystals of Fo90 and Fo57 olivines dissolve to iron-rich melt derived from melting of fayalite. The dissolution of relict crystals produce steep chemical gradient at interface between crystals and melt. Melting kinetics of Fo90 olivine produces quite characteristic projections from the surface of spherules.

Textures of quench growth olivine on relict crystals resemble to hourglass shape. Compositions of the quench crystals range between Fo50 and Fo20. Solidus temperatures of olivine in this compositional range may keep supercooling in quenching processes.

Keywords: Olivine, melting textures, nucleation, crystal growth, dendrites, quench textures

Molecular dynamics simulations of oil wettability of muscovite-NaCl solution interface

KOBAYASHI, Kazuya^{1*} ; LIANG, Yunfeng¹ ; MATSUOKA, Toshifumi¹ ; NISHI, Naoya¹ ; SAKKA, Tetsuo¹

¹Graduate School of Engineering, Kyoto University

The investigations of the properties of mineral-electrolyte solution-oil interface are of importance for developments of resources and underground disposals of toxic wastes. The behavior of electrolytes at mineral-electrolyte solutions (e.g. formation of electric double layer) changes their properties. It is known that the wettability of mineral surface by oil in aqueous solutions depends on the concentration of the electrolytes. However, the fundamental relationship between the change in wettability and the behavior of electrolytes has not been revealed. Therefore, we applied molecular dynamics simulation, which provides nano-scale interfacial structure and dynamics of molecules, in order to investigate the mineral-electrolyte solution-oil interfacial structure and wettability. The muscovite, 3.0 mol/kg NaCl aqueous solution, and heptane or toluene were used as mineral, electrolyte solution, and oil, respectively. The simulations revealed that the adsorption of Na⁺ at negatively charged muscovite surface decreases the interfacial tension at mineral-aqueous solution interface whereas negative adsorption of electrolytes increases the interfacial tension at oil-electrolyte solution interface for both the oil molecules. The changes in the two interfacial tensions alter the wettability of oil droplets. This research provides the fundamental knowledge for applications to enhanced oil recovery.

Keywords: Muscovite, Mineral-underground fluid interface, Wettability, Molecular dynamics

High-pressure Raman spectroscopic studies of hydrogarnet, katoite $\text{Ca}_3\text{Al}_2(\text{O}_4\text{H}_4)_3$

KATO, Masato^{1*}; KYONO, Atsushi²

¹Graduate School of Life and Environmental Sciences, University of Tsukuba, ²Graduate School of Life and Environmental Sciences, University of Tsukuba

Because garnet is capable of incorporating small concentrations, a lot of attention has been devoted to the hydrogarnet known as nominally anhydrous minerals (NAMs). The calcium garnet exhibits the complete solid solution between grossular $\text{Ca}_3\text{Al}_2(\text{SiO}_4)_3$ and Si-free katoite, hydrogarnet $\text{Ca}_3\text{Al}_2(\text{O}_4\text{H}_4)_3$. Lager et al. (2002) suggested that in the katoite a phase transition occurred from space group $\text{Ia}\bar{3}\text{d}$ to I-43d which is a non-centric subgroup of $\text{Ia}\bar{3}\text{d}$ with increasing inter-tetrahedral H H repulsion.

We report in situ Raman spectroscopic studies of katoite in a diamond-anvil cell under hydrostatic conditions up to 10 GPa at room temperature. The vibration modes observed in the study were analyzed theoretically by factor group analysis. Three bands near 332 and 537, 3652 cm^{-1} were observed clearly at 1.0 GPa. In the wavenumber region of lattice modes, the lower frequency peak was assigned to a mode of $\text{E}_g + \text{F}_2g$ symmetry and the higher frequency peak was assigned to a mode of $\text{A}_1g + \text{F}_2g$ symmetry. In the OH stretching vibration region, the peak was assigned to $\text{A}_1g + 2\text{E}_g + 3\text{F}_2g$ symmetry. The peak positions and shapes in the Raman spectra agree well with those measured under ambient conditions. The pressure dependences of the lattice modes and the OH stretching vibration mode show a positive and negative pressure shifts, respectively. A shorter (and so stronger) hydrogen bond is well known to have lower frequencies than a weaker hydrogen bond (Nakamoto et al., 1955), therefore the negative pressure shift observed in the study indicated that the hydrogen bonding strength in katoite was increased as a function of pressure. Peak shift of the OH stretching vibration mode showed different trends at pressure above 5 GPa. Increasing rate of full width half maximum (FWHM) for lattice mode was varied at 6 GPa.

When the phase transition in katoite occurs from space group $\text{Ia}\bar{3}\text{d}$ (point group O_h) to I-43d (Td) at about 5 GPa (Lager et al., 2002), the vibration modes are never splitted with the phase transition. On the other hand, when the symmetry changes from O_h (cubic) to D_4h (tetragonal), the E_g and F_2g modes split to $\text{A}_1g + \text{B}_1g$ and $\text{B}_2g + \text{E}_g$, respectively. Therefore the expansion of FWHM above 6 GPa is interpretable as the cubic-tetragonal transition. The results in the study indicate that in katoite structural phase transition occurs from cubic to tetragonal at about 6 GPa.

Keywords: katoite, high-pressure Raman spectroscopy, phase transition

Physical properties of methane hydrate under low temperature and high pressure

HIRAI, Hisako^{1*}; TANAKA, Takehiko¹; HIRAO, Naohisa²; OHISHI, Yasuo²; YAMAMOTO, Yoshitaka³; OHTAKE, Michika³; IRIFUNE, Tetsuo¹

¹Geodynamics Research Center, Ehime University, ²JASRI, ³AIST

Methane hydrate, called fiery ice, has the potential to become an important energy resource in the future. It is also thought to be an important constituent of icy planets like Neptune and satellites such as Titan, thus making it an important part of planetary science. Methane hydrate is known to exhibit an sI structure at low pressures and room temperature, and transforms to an sH cage structure at approximately 0.8 to 1.0 GPa. A further transformation to a filled-ice Ih structure (FIHs) occurs at approximately 1.8 to 2.0 GPa, with this structure consisting of an ice framework similar to ice Ih that contains voids filled with methane molecules. The guest methane molecules are rotation freely in the ice framework. The FIHs has been reported to survive up to 86 GPa at room temperature with two phase change. However, phase changes and properties at low temperatures and high pressures have not been studied so far. This study intended to clarify the changes in phase and properties of FIHs of methane hydrate.

High pressure and low temperature experiments were performed using clamp-type diamond anvil cells and a helium-refrigeration cryostat. The pressure and temperature conditions were 2.0 to 77.0 GPa and 30 to 300 K, respectively. As the initial materials light-water host sample and deuterated-water one were used.

In situ X-ray diffractometry and Raman spectroscopy revealed existence of three phases and the phase boundaries between them. The first phase is guest orientationally disordered phase, i.e. well-known FIHs, which exists below 20 GPa, the second one is guest orientational ordering phase above 20 GPa, and the third one is another guest ordering phase with different ordering manner. The results demonstrate that phase changes of methane hydrate proceed via proceeding of guest orientational ordering. However, it seemed a quite peculiar that the slopes of phase boundary are negative. Another low temperature experiments performed revealed the volume expansion at low temperature below 150- 100 K. The expansion was confirmed not due to non-hydrostatic effect but to be intrinsic by annealing treatment. The peculiar phenomenon were examined considering to host proton ordering.

Keywords: Methane hydrate, Low temperature and high pressure, Guest orientational ordering, Volume change

Change in fayalites with ultraviolet rays and water

KOMORI, Nobuo^{1*}

¹Kamata junior high school

I reported a change in quality of the fayalite from Hachijojima with ultraviolet rays and the water in this meeting two years ago. I did similar experiment with fayalite from Kawamata-machi, Fukushima afterwards.

I purchased these Fayalites from two companies (company A and company B).

These Fayalites were done the ultrasonic cleaning with tap water and distilled water.

The fayalite of company A has weak degree of the weathering in the outdoors.

The fayalite of company B has more intence degree of the weathering in the outdoors than company A. I decided that the fayalite of company A is called sample A and tha fayalite of company B is called sample B. I carried out following experiment using sample A and sample B.

One of sample B which weight is about 2g, are put in the test tube filled with distilled water. The test tube is irradiated with ultraviolet rays with their peak wave length of 254 nm. Another experiment was done as a comparison under the same condition but without ultraviolet. The tubes were irradiated with ultraviolet rays for three months. The illuminance of ultraviolet rays is 40w/m²when the experiments were first strated.

As a result of this experiment, a lot of brown powder was generated in the test tube that was irradiated with ultraviolet rays. It was estimated by XRD analysis that the brown powder might include Fe₂O₃,FeO (OH),MnO₂.

However, the tube without ultraviolet rays irradiation generated no powder. And I did the same experiment using sample A. As a result no brown powder was generated in the test tube that was irradiated with ultraviolet rays and was not irradiated too.

About these result I estimated as follows.

Because the sample B had much quantity of iron ion in the water and the oxidation of iron ion was promoted by ultraviolet rays, so a lot of powder of the iron oxide was produced in water. Because the sample A had very little iron ion in water,so iron oxide hardly occurs.

Keywords: ultraviolet rays, water, fayalite, iron oxide, maghemite, change

Carbon dissolution mechanism in forsterite

MITANI, Saki^{1*}; KYONO, Atsushi¹

¹Graduate School of Life and Environmental Sciences, University of Tsukuba

Introduction

Silicates are major and important minerals that constitute the Earth's crust and mantle. An enormous amount of carbon is also contained in the Earth's interior. Shcheka et al. (2006) studied about carbon solubility in mantle minerals by high temperature and high pressure experiments, and indicated that carbon solubility increases as a function of pressure to a maximum of ~12 ppm by weight in olivine at 11 GPa. In this case, carbon substitutes as C^{4+} for Si^{4+} and occupies SiO_4 tetrahedra as CO_4 tetrahedra. Sen et al. (2013) suggested that significant substitution of C^{2-} for O^{2-} could occur in geological silicate melts/glasses at moderate pressure and high temperature and might be thermodynamically far more accessible than C^{4+} for Si^{4+} substitution. Thus, it has not been perfectly obvious whether carbon substitutes for Si^{4+} and create CO_4 tetrahedra or substitutes for O^{2-} partially and create $Si(O,C)_4/SiC_4$ tetrahedra.

In this study, we determined the carbon dissolution mechanism in forsterite, which is the major minerals in the upper mantle.

Experimental method

Natural forsterite (San Carlos, California, USA) was used in carbon solubility experiments. Forsterite was mixed with either graphite as a crystalline solid or activated carbon as an amorphous form to be homogenized powder. Then, they were heated for 1000 °C, 2 days under ambient pressure. After that, the X-ray powder diffraction study was performed to analyze the change of lattice parameters of the reaction products. The FT-IR study was performed to indicate whether carbon dissolved in SiO_4 tetrahedra. The EPMA analysis was for quantitative analysis of carbon in the reaction products. Moreover, assumption of the reaction product structures was done by the first-principle calculation.

Result and discussion

The X-ray powder diffraction study showed that as increasing the carbon content, the lattice parameters were isotopically contracted. The FT-IR study showed that a C-O bond would be partially formed. Moreover, the EPMA analysis revealed that a small amount of carbon was dissolved in the forsterite with a negative correlation between Si and C. All of the experimental results obtained so far suggested that carbon was able to dissolve in the SiO_4 tetrahedra in forsterite as C^{4+} . The first-principle calculation supported the observed results and the proposed substitution model in the study.

However, the quantity of carbon dissolution in forsterite is low, so we have to repeat verification experiments carefully and lead the conclusion.

Keywords: silicate mineral, carbon dissolution, forsterite

Viscosity of KAlSi_3O_8 melt under high pressure

SUZUKI, Akio^{1*}

¹Tohoku University

Viscosity is a fundamental property controlling the transportation of magma in the planetary interiors. In this study, we measured the viscosity of KAlSi_3O_8 composition of melt under high pressure. The viscosity was measured by the falling sphere method using an X-ray radiography system. Experiments were performed at the NE7A station of the PF-AR synchrotron radiation facility in KEK, Tsukuba, Japan. High pressure was generated using a Kawai-type apparatus driven by a DIA-type guide block in the MAX-III press. A powder of natural sanidine (KAlSi_3O_8) was loaded with a platinum sphere in a molybdenum container. Powder X-ray diffraction data were obtained by energy-dispersive method using a pure Ge solid state detector. Pressures were determined by using an equation of state of MgO. The results show that the viscosity of KAlSi_3O_8 melt decreased with increasing pressure up to 6 GPa.

Keywords: magma, viscosity, high pressure, mantle, synchrotron radiation

Elastic constants of single-crystal quartz and their temperature dependence studied via sphere-resonance method

SEMA, Fumie^{1*} ; WATANABE, Tohru¹

¹Graduate School of Science and Engineering, University of Toyama

Single-crystal elastic constants of rock-forming minerals and their temperature dependence are critical for interpreting observed seismic velocities. A good interpretation requires a thorough understanding of elastic properties of major constituent minerals. Compared with mantle minerals such as olivine, to which a lot of work have been done, elastic properties of crustal minerals have been poorly constrained. Quartz is one of the most abundant minerals in the crust. We have studied elastic constants of single-crystal quartz and their temperature dependence by the sphere-resonance method.

A sphere sample ($D=5.826(1)$ mm) was made from a synthetic quartz single-crystal by the two-pipe method. Resonant frequencies were measured with ultrasonic transducers (Panametrics, V156RM), a lock-in-amplifier (SRS, SR844) and a function generator (Tektronix, AFG320). Measurements were made at frequencies from 400 kHz to 1.2 MHz with different specimen-holding forces. Extrapolating to the specimen-holding force of zero, we obtained frequencies of "free" oscillation. The sample and transducers were placed in a temperature-controlled container. The temperature was changed from 0 to 40°C. Elastic constants were determined by comparing measured and calculated resonant frequencies. The xyz algorithm (Visscher et al., 1991) was employed to calculate resonant frequencies of the sphere sample. Preliminary analysis has shown that C_{11} , C_{33} , C_{44} , C_{12} , C_{13} and C_{14} at room temperature (19.4°C) are 87.224, 105.47, 58.328, 6.885, 11.914, 18.116 (GPa), respectively. The temperature dependence of elastic constants will also be presented in this poster.

Keywords: elastic constants, resonance method, temperature dependence, quartz

A kinetical study of proton dynamics of brucite and portlandite

MASUDA, Manami¹ ; NAGAI, Takaya^{2*} ; KAWANO, Jun²

¹School of Science, Hokkaido University, ²Faculty of Science, Hokkaido University Graduate

Brucite is $Mg(OH)_2$ compound and the crystal structure of brucite is recognized as a prototype of hydrous layered minerals with complicated structures. Various physical and chemical properties of some minerals with the brucite structure such as brucite itself and portlandite, $Ca(OH)_2$ have been investigated. It is especially interesting to understand proton dynamics in hydrous minerals, because the proton diffusion should be closely related to mechanism and kinetics of plastic deformation, hydration, dehydration and so on. Nevertheless, proton diffusion studies on brucite structured minerals have been surprisingly scarce. Recently Noguchi and Shinoda (2010) conducted H-D exchange diffusion experiments on portlandite and Guo et al.(2013) performed proton diffusion experiments on brucite at high pressure. However, it is difficult to understand mechanism of proton diffusion of brucite structured minerals systematically, because their experimental conditions such as pressure and temperature are different. In this study, we performed deuterated experiments for brucite, hydrated experiments for deuterated brucite and deuterated experiments for portlandite at several temperatures and at an atmospheric pressure.

All sample powders were prepared by hydrothermal synthesis and checked the qualities by X-ray diffraction, infrared absorption spectroscopy and SEM. The H-D exchange experiments at several temperatures were performed with a vertical tube furnace in which bubbling dried N_2 gas through D_2O (or H_2O) was introduced. A crucible filled with the sample powder was hung in the middle of the tube furnace. A small amount of the sample powder was picked out at appropriate time intervals and IR measurements for it were performed to know time variation of the molar ratio of D to H.

The diffusion rate depends on temperature and is faster at higher temperature. The diffusion rate also depends on the molar ratio of D to H. Rate control process of proton diffusion in brucite structured minerals will be discussed from diffusion coefficients, activation energies and frequency factors determined.

Keywords: Proton dynamics, H-D exchange, brucite, portlandite, kinetics

Application of the Raman carbonaceous material thermometer to chondrites

HOMMA, Yoshitaka^{1*}; KOUKETSU, Yui¹; KAGI, Hiroyuki¹; MIKOUCHI, Takashi¹; YABUTA, Hikaru²

¹Graduate School of Science, The University of Tokyo, ²Graduate School of Science, Osaka University

Introduction

Structure of carbonaceous material (CM) reflects the experience of thermal metamorphism which occurred on their parent bodies. Therefore, various applications of CM to geothermometer on both terrestrial metasediments and primitive chondrites have been reported so far. Raman spectroscopy is a promising method to investigate the structure of CM, because of the in-situ, non-destructive analysis. Raman spectra of CM have characteristic bands at around 1600cm^{-1} (G-band) and 1355cm^{-1} (D1-band). Recently, detailed analysis on Raman spectra of CM using four or five peaks on terrestrial metasediments extended the applicable range of thermometer to $150\sim 650\text{ }^{\circ}\text{C}$ (Kouketsu et al., 2014). On the other hand, only two peaks are applied in the regression analysis on Raman spectra of CM in meteorites at present. In this research, we try to improve the Raman thermometer on CM in meteorite by applying the detailed peak fitting method.

Samples and Methods

In this research, 20 samples were chosen from carbonaceous chondrites, ordinary chondrites and R chondrites. Raman spectra were obtained on CM in 14 bulk meteorites, thin section of five samples and insoluble organic matter (IOM) extracted from one sample. Laser power at the sample surface was controlled in the range of $1\sim 2.5\text{ mW}$, and acquisition time was $10\sim 30\text{ s}$. For most of the samples, at least 30 data sets were acquired. After removing the background by a linear baseline, the obtained spectra were fitted by four pseudo-Voigt functions.

Results and Discussion

Four-peak spectral fitting (using G_L , D1, D3 and D4-band) was performed on each sample. The result suggested that there is a correlation between the full width at half maximum (FWHM) of D1-band and peak metamorphic temperatures (PMT). A calibration curve was obtained by using seven samples whose metamorphic temperature were already estimated to be $120\sim 550\text{ }^{\circ}\text{C}$ in the previous study (Huss et al., 2006). The derived relationship between the FWHM of D1-band (Γ_{D1}) and PMT is represented by a liner function.

To verify whether the obtained thermometer is applicable to other chondrites, we observed the relationship between Γ_{D1} and other parameters. The relationship between intensity ratio I_{D1}/I_{GL} and Γ_{D1} showed that the value of Γ_{D1} has the lowest limit. This phenomenon was also identified in Kouketsu et al. (2014). From the obtained results, the upper limit of the thermometer was found to be ($550\text{ }^{\circ}\text{C}$).

Conclusion

This study revealed that Raman thermometer on CM is applicable to estimate the metamorphic temperature of primitive chondrites by using the FWHM of the D1-band. The relational is expressed by a linear function and the applicable temperature range is $200\text{ to }550\text{ }^{\circ}\text{C}$. There is a possibility to apply this thermometer to the low metamorphic region under $200\text{ }^{\circ}\text{C}$ by increasing assay samples, although there is still room to optimize the fitting conditions.

Keywords: chondrites, carbonaceous material, Raman spectroscopy, thermal history

Nature of Si-O bonding via molecular orbital calculation

NORITAKE, Fumiya^{1*} ; KAWAMURA, Katsuyuki¹

¹Okayama University

Understanding the nature of Si-O bonding and Si-O-Si bridging is important for mineralogy, material science and metallurgy. It is well known that the variation of Si-O-Si angle in silicates is caused by difference of composition, temperature and pressure. The change of angle of Si-O-Si bridging affects the strength of Si-O bonding. For instance, the increase of Si-O-Si angle decreases the Si-O bond length in coesite crystal (Gibbs et al. 1977). The decrease of Si-O-Si angle of liquid silicates as a result of compression is reported by various researchers (e.g. Navrotsky et al., 1985 Ohtani et al., 1985, Sakamaki et al., 2012). The decrease of Si-O-Si angle is thought to be the trigger of decrease of viscosity of liquid silicates. (Navrotsky et al., 1985, Noritake et al., 2012). Quantum chemical properties of Si-O-Si bridging is investigated to understand the relationship between Si-O-Si angle, Si-O bond length and its strength (e.g., Newton and Gibbs 1980, Tsuneyuki 1996, Kubicki and Sykes 1993). Newton and Gibbs (1980) reports the pyrosilicic acid molecule has energy minimum at Si-O-Si angle of 145 ° using STO-3G basis set (Hehre et al 1969) by Hartree-Fock method. Tsuneyuki (1996) reports that the bending of Si-O-Si is not reproduced using double-zeta function basis set nevertheless the increase of the number of basis function generally increase the reproducibility. However, the nature of Si-O-Si bridgings seems not to be reproduced by increase of basis function using Hartree-Fock method. In this paper, we show the molecular orbital calculation about pyrosilicic acid molecule using post-Hartree-Fock method and more precise basis set to understand the nature of Si-O-Si bridging.

Molecular orbital calculations were performed using the GAUSSIAN 09 code. We firstly calculate the optimized structure of disiloxane (Almenningen et al., 1963) by Hartree-Fock (HF), second-order Moller-Plesset perturbation theory (MP2), and two density functional theory (Becke's density functional (Becke, 1988) with three correlation functionals by Lee, Yang and Parr (B3LYP) (Lee et al., 1988), and generalized gradient approximation by Perdew, Burke and Ernzerhof (PBE) (Perdew et al., 1996)) with 6-311G(d,p) split valence double zeta basis set (Raghavachari et al., 1980). The bending of Si-O-Si bridging is not reproduced by HF method as shown in Tsuneyuki (1996). The bending of Si-O-Si bridging is reproduced by use of MP2 and density functional theory with PBE. The optimized angle of Si-O-Si in disiloxane molecule by MP2 is closer to experimental value than that by PBE. Then we apply the MP2 method with 6-311G(d,p) basis set to the calculation of pyrosilicic acid, H₆Si₂O₇. NBO analysis (Foster and Weinhold, 1980, Reed et al., 1985; 1988) is used to analyze the electronic state of bonding.

We found the equilibrium geometries for bended two pyrosilicic acid molecules (C_{2v} and 60 ° torsion) using Moller-Plesset perturbation theory and with 6-311G(d,p) split valence double zeta basis set. We calculated the energy surface with varying Si-O_{br} length and Si-O-Si angle and found the relationship between Si-O_{br} length and bridging angle. From the energy surface, the stable Si-O bond length decrease with spreading Si-O-Si angle. The bending of Si-O-Si angle in equilibrium geometries can be explained by explained by the balance of Coulombic repulsion between tetrahedra and lone pair electrons of bridging oxygen atom without concerning the contribution of d-p π-bonding. The Si-O bonding strengthen with increasing Si-O-Si angle because of stabilization in energy of Si-O bonding orbital with decreasing the hybridization index λ in sp^λ orbital of bridging oxygen and increase of coulombic interaction between Si and bridging oxygen atom.

Keywords: Molecular orbital calculation, Si-O-Si bridging

Bule cathodoluminescence derived from defecte centers in magnesite

KUSANO, Nobuhiro^{1*} ; NISHIDO, Hirotsugu¹ ; NINAGAWA, Kiyotaka¹

¹Okayama University of Science

Cathodoluminescence (CL) has been widely applied in mineralogical and petrological investigations, especially for carbonates. Although most calcite-type carbonates exhibit red to orange CL activated by divalent Mn ions, blue CL is uncommon in carbonates, but not with bright emission (e.g., Machel et al., 1991). Magnesite occasionally shows red CL emission assigned to an impurity center of divalent Mn ion substituted for an Mg ion as an activator (Medlin 1963, Sommer 1972), but not usually accompanied by blue emission. We have confirmed a significant blue emission in the CL of magnesite from Tennohama, Wakayama, Japan.

Blue luminescent magnesite (BM) occurs as a rhombohedral crystal in hydrothermal veinlets associated with dolomite and quartz. Its single crystal in size of 2-3 mm has been employed for CL measurements, as well as a single crystal of common magnesite (RM) with red CL emission from Brumado, Brazil. Color CL images were obtained using a cold-cathode type Luminoscope with a cooled-CCD camera. CL spectroscopy was made by a SEM-CL system, which is comprised of SEM (JEOL: JSM-5410LV) combined with a grating monochromator (OXFORD: Mono CL2). The CL emitted from the samples was dispersed by a grating monochromator (1200 grooves/mm), and recorded by a photon counting method using a photomultiplier tube. All CL spectra were corrected for total instrumental response, which was determined by use of a calibrated standard lamp.

BM spectrum shows an enhanced broad-band emission with triplet peaks from 300-400 nm in a blue region and a broad-band emission at ~670 nm in a red region, whereas RM has an intense broad band emission at ~670nm previously reported in magnesite samples (e.g., Sommer, 1972) and no emission in a blue region. Blue CL emissions of BM is possibly to be the "background blue" found in the calcite contained almost no activator (Richter and Zinkernagel, 1981), which might be related to an intrinsic defect center. In the case of BM, its emission band in a blue region has triplet peaks with high intensity, but a single broad band with low intensity for calcite.

Therefore, a Gaussian fitting of BM spectrum in an energy unit successfully deconvolutes three emission components at around 2.52 eV (492 nm), 3.28 eV (378 nm) and 3.88 eV (320nm) in a blue region. Kusano et al. (2014) reported a blue CL emission in the calcite with emission components at 2.67eV (464nm) and 3.30eV (376nm), which is the material decomposed from dolomite in the process of skarn mineralization at high temperature. It suggests that the CL derived from defect centers in BM might be attributable to its thermal history during crystal growth.

Keywords: magnesite, cathodoluminescence, blue emission, defect center

Cathodoluminescence characterization of enstatite in meteorites.

OHGO, Syuhei^{1*} ; NISHIDO, Hirotsugu¹ ; NINAGAWA, Kiyotaka¹

¹Okayama University of Science

Enstatite in meteorites occasionally shows various cathodoluminescence (CL) emissions with red, reddish purple and blue, whereas terrestrial enstatite has almost no CL emission. We have confirmed several luminescent enstatite in enstatite chondrite (E-chondrite) and enstatite achondrite (Aubrite). In this study, we have conducted to clarify the luminescence centers of CL emissions in extraterrestrial enstatite compared to the CL of terrestrial enstatite.

The polished thin sections of E-chondrites (Sahara 97096, Sahara 97121, Dar al Gani 734 and Y 86004) and Aubrite (Al Haggounia 001) were used for CL measurements. Color CL images were obtained using a cold-cathode type Luminoscope with a cooled-CCD camera. CL spectroscopy was made by a SEM-CL system, which is comprised of SEM (JEOL: JSM-5410LV) combined with a grating monochromator (OXFORD: Mono CL2). The CL emitted from the samples was dispersed by a grating (1200 grooves/mm), and recorded by a photon counting method using a photomultiplier tube. All CL spectra were corrected for total instrumental response, which was determined using a calibrated standard lamp.

Color CL imaging reveals various types of CL emissions with red, reddish purple and blue in the extraterrestrial enstatite. The CL spectra of these enstatite show a broad emission band at 670 nm in a red region, which is assigned to an impurity center derived from activated divalent Mn ion substituted for Mg, and a broad emission band at around 400 nm in a blue region, which might be related to a defect center possibly assigned to "intrinsic defect center" derived during crystal growth.

CL spectra were converted into energy units for spectral deconvolution using a Gaussian curve fitting, because one Gaussian curve in energy units should correspond to one specific type of emission center (Stevens-Kalceff, 2009). The deconvoluted components can be assigned to the emission centers related to impurity centers of trivalent Cr ion at 1.64 eV and divalent Mn ion at 1.86 eV and two defect centers at 2.71 and 3.18 eV. The emission component at 3.18 eV might be attributed to the defect center of structural distortion by the substitution of Al ion for Si in a tetrahedral site, which is possible to be in the process of crystal growth at high temperature in its parent body (e.g., the rocks hosting Al-rich enstatite formed at depths from 25 km to 130?200 km in the lunar rock; Nazarov et al., 2011). Al contents in blue luminescent enstatite are higher than that in red luminescent one. Blue emission center can be detected in the CL of terrestrial samples.

Keywords: Enstatite, Cathodoluminescence, E-chondrite, Emission center

Self-diffusion of hydrogen in high-pressure ices: Preliminarily results

NOGUCHI, Naoki^{1*} ; OKUCHI, Takuo¹ ; TOMIOKA, Naotaka²

¹Institute for Study of the Earth's Interior, Okayama University, ²Japan Agency for Marine-Earth Science and Technology

High-pressure ices are the primary constituents of mantles of the large icy bodies such as some of Galilean satellites and Edgeworth-Kuiper Belt Objects. Understanding self-diffusion of hydrogen in these high-pressure ices is essential to discuss about mantle dynamics of the large icy bodies because it controls rheology of these ices. In addition, diffusive properties of high-pressure ices are also an interesting topic in the field of high-pressure material science. Shortening of intermolecular distance with increasing pressure induces drastic changes of hydrogen-bonding property such as proton tunneling, proton symmetrization (Benoit et al. 1998), hydrogen sublattice melting (Cavazzoni et al. 1999), and proton hopping transition (Noguchi et al. 2014). Whether these changes of hydrogen bonding affect hydrogen diffusion or not is a major subject in the proton dynamics at high pressure. To elucidate these questions, we have carried out an experiment to determine hydrogen diffusion coefficients of the high-pressure ices using a diamond anvil cell (DAC) and Raman spectroscopy.

The diffusion couples have been prepared from polycrystalline H₂O and D₂O ices prepared within a sample chamber of DAC. The diffusion experiments of these couples were carried out using an electric furnace. Temperatures were set in a range between 400 K and 500 K. After keeping the DAC in the furnace for a few days, Raman mapping measurements of the diffusion couples were carried out at room temperature. Two-dimensional diffusion profiles of deuterium were determined using quantitative curves for deuterium concentration. The quantitative calibration curves were functions as the relative area of Raman band of OH stretching mode to that of OD stretching mode, or Raman shifts of OH and OD stretching modes. Preliminarily results will be reported in our presentation.

Keywords: high-pressure ices, self-diffusion, rheology, Raman spectroscopy

Structure investigation of mordenite induced by molecular sieve using the Rietveld method

SUGANO, Neo^{1*}

¹Life & Env. Sci. Univ. of Tsukuba

[Introduction]

There are a large number of natural and synthesis zeolite minerals that are generally composed of Si/AlO₄ three-dimensionally framework structure. All of them have a porous structure that can adsorb water molecules in their micropores. In addition, zeolite minerals have the highly adsorption and preservation properties generally called molecular sieve that accommodate a variety of cations and molecules in the micropore due to the negative electric charge caused by the substitution of Al₃⁺ for Si₄⁺. The high cation exchange ability has been received great attention in many fields.

Mordenite [(Na₂, Cs, K₂)₄(Al₁₈Si₄₀)O₉₆·28H₂O] (Martucci et al., 2003) is well known for its high selectivity for radioactive Cs and Sr. However, there are only few studies that addressed the crystal structural change of mordenite by Cs⁺-ion exchange molecular sieve. Hence, this study is aimed to clarify the relationship between molecular sieve and structural change of mordenite.

[Experimental Methods]

The structural change of mordenite were investigated by the Rietveld refinement analyses based on the powder X-ray diffraction measurements; CuK α ($\lambda = 1.54056 \text{ \AA}$), $5^\circ \leq 2\theta \leq 120^\circ$, scanning speed = $4^\circ/\text{min}$, scanning width = 0.02° . Cs-exchanged mordenite were prepared from H-mordenite by ion exchange in CsCl solutions with various Cs concentration (0.010, 0.10, 1.0, 2.0, 4.0, 8.0, 10.0, 30.0g/l). Cs-exchange experiments were executed by the shaking (32rpm) for 48hrs. The temperatures of solutions were maintained around 20°C.

[Results and Discussion]

The pH value of the solutions was initially 3.44 ± 0.02 , but it was decreased to $2.70-3.09 \pm 0.02$ with addition of mordenite. The decreasing of pH value with the Cs concentration indicated that Cs⁺-ion was substituted for H⁺-ion within the micropore of mordenite structure. Consequently, the lattice parameter of mordenite was isotropically decreased with the Cs⁺-ion concentration. The unit cell volume of mordenite was slightly decreased from 2880 (12) \AA^3 to 2836 (12) \AA^3 (at most 44 (17) \AA^3).

The molecular sieve of mordenite was characterized by the contraction of 12-membered ring channel (12MRc) and 8-membered ring channel (8MRc) where the Cs⁺-ion can be accommodated within the mordenite structure. The 12MRc with the largest pore size was appropriately contracted with the Cs content due to the electrostatic attraction between Cs⁺-ion and framework atoms. The contraction of 12MRc (at most 0.31(8) \AA) especially acted toward the direction of b-axis. The high absorption efficiency of the molecular sieve is caused by the site preference of Cs⁺-ion into the 12MRc. The 8MRc with the smaller pore size than the 12MRc directly connected with the 12MRc. It behaves in the opposite way to the 12MRc. The 8MRc is strongly affected with the structural modification of 12MRc. Since the Cs⁺-ion are hardly incorporated into the 8MRc, the site occupancy of Cs⁺-ion in the 8MRc is always lower than that in 12MRc, which leads to the small contraction values of 8MRc.

Keywords: Mordenite, Molecular sieve, Rietveld refinement

In situ high pressure IR spectroscopic observations on the upper mantle anhydrous minerals using diamond anvil cell

SAKURAI, Moe^{1*} ; TSUJINO, Noriyoshi² ; TATENO, Shigehiko³ ; SUZUKI, Toshihiro¹ ; YOSHINO, Takashi² ; KAWAMURA, Katsuyuki⁴ ; TAKAHASHI, Eiichi¹

¹Earth and Planet. Sci., Tokyo Tech, ²ISEI, Okayama Univ., ³ELSI, Tokyo Tech., ⁴Environmental and Life Sci., Okayama Univ.

Most nominally anhydrous minerals (NAMs) in the Earth's upper mantle can contain small amounts of hydrogen (i.e. "water"), structurally bond as hydroxyl. Structurally bounded water causes important influences on many physical properties of mantle rocks. The influence seems to be controlled by hydrogen atoms positions in crystal structure. In most of previous researches, hydrogen atoms positions have been estimated by comparison between the theoretically calculated IR spectra and the experimental results, which obtained at ambient pressure [1, 2]. Therefore, the influence of pressure on hydrogen atom positions has not been identified yet. However, the physical properties relating to hydrogen atom (electric conductivity, viscosity and more), have been measured at high pressure conditions. Thus it is important to clarify the influence of pressure on hydrogen atoms positions.

To observe the influence of pressure on IR spectra, high-pressure experiments have been conducted at pressures of 0.4 – 9.0 GPa at room temperature. The experiments were performed with diamond anvil cell by using natural olivine (Ol) and synthetic forsterite (Fo) as starting materials. The pressure medium was KBr powder or fluorinert. Pressure was determined by ruby fluorescence method [3]. The IR spectra were obtained with a vacuum type Fourier transform infrared spectrometer (Jasco: FT-IR6100, IRT5000).

Clear OH stretching vibration bands could be observed for samples with water concentration over ~100 wt.ppm. The non-polarized IR spectrum of synthesized Fo showed four bands; two stronger ones at 3610, 3575 cm⁻¹ and two weaker bands at 3550, 3475 cm⁻¹ at ambient pressure. The band at 3475 cm⁻¹ disappeared in the spectrum of randomly oriented Fo at ≥5.6 GPa. The band at 3610 cm⁻¹ shifted to low wavenumber with increasing pressure. After decompression, the spectrum return to the almost same position and intensity before increasing pressure. Thus it indicates that these bands shift is a reversible change.

The polarized to *a*-axis IR spectrum of natural Ol showed three bands; 3610, 3598 and 3575 cm⁻¹ at ambient pressure. The band at 3610 cm⁻¹ shifted to low wavenumber and became weaker with increasing pressure. The band at 3575 cm⁻¹ shifted to high wavenumber, which results is opposite to the band at 3610 cm⁻¹, and also became weaker with increasing pressure. The polarized to *b*-axis IR spectrum of natural Ol showed two bands; 3598 and 3575 cm⁻¹. The band at 3598 cm⁻¹ did not change with increasing pressure. In this experiment, the diamond anvils touched sample directly above 8 GPa, so we could not observe the spectrum after decompression.

[1] Umemoto et al.: *Am. Min.*, 96, 1475-1479, 219 (2011) [2] Sakurai et al.: *J. Comput. Chem. Jpn.* [3] Mao et al.: *J. Appl. Phys.* 49, 3276-3283 (1978)

Keywords: FT-IR, Pressure effect, Nominally anhydrous minerals, Upper mantle, In situ experiment

Study on the stability of the $\text{Al}_{65}\text{Cu}_{20}\text{Fe}_{15}$ icosahedral quasicrystal using Synchrotron X-ray diffraction method

TAKAGI, Sota^{1*} ; KYONO, Atsushi²

¹College of Geoscience, School of Life and Environmental Sciences, University of Tsukuba, ²Graduate School of Life and Environmental Sciences, University of Tsukuba

The stability of the $\text{Al}_{65}\text{Cu}_{20}\text{Fe}_{15}$ icosahedral quasicrystal at high pressure and high temperature has been investigated using synchrotron X-ray diffraction method. High pressure *in situ* XRD experiments were performed up to 104 GPa, and high pressure and high temperature *in situ* XRD experiments were performed at the pressure points of 11, 24, 33, 57, 67, 104 GPa up to temperature of about 2500 K. The high pressure experiments revealed that five characteristic XRD peaks of the $\text{Al}_{65}\text{Cu}_{20}\text{Fe}_{15}$ icosahedral quasicrystal remained up to 104 GPa at room temperature, while a new peak appeared at the point of $d = 2.90 \text{ \AA}$ above 89 GPa. The six-dimensional lattice parameter, a_{6D} , was continuously contracted from 12.5 \AA to 11.2 \AA with pressure. The bulk modulus of the $\text{Al}_{65}\text{Cu}_{20}\text{Fe}_{15}$ icosahedral quasicrystal started to change around 70 GPa. This result suggested that the $\text{Al}_{65}\text{Cu}_{20}\text{Fe}_{15}$ icosahedral quasicrystal was transformed to high pressure phase at about 70 GPa. The high pressure and high temperature experiments showed that a different phase (high-temperature phase) occurs as a function of the temperature. The phase boundary between the $\text{Al}_{65}\text{Cu}_{20}\text{Fe}_{15}$ icosahedral quasicrystal and its high temperature phase was risen with pressure, such as 865 K at 11 GPa, 1402 K at 24 GPa, 1758 K at 33 GPa, 1963 K at 57 GPa, 2050 K at 67 GPa, 2080 K at 104 GPa. In a series of the study, the $\text{Al}_{65}\text{Cu}_{20}\text{Fe}_{15}$ icosahedral quasicrystal was melted completely only when it was heated to 2385 K at 11 GPa. From the present study, it was suggested that mineral icosahedrite ($\text{Al}_{63}\text{Cu}_{24}\text{Fe}_{13}$), the first natural-occurring quasicrystal, was formed at pressure range from 5 GPa to 70 GPa, and at temperature range from 1500 K to 2200 K. This study can be a clue to solve the question of where and how the icosahedrite was formed.

Keywords: $\text{Al}_{65}\text{Cu}_{20}\text{Fe}_{15}$ icosahedral quasicrystal, icosahedrite, stability, high pressure and high temperature, XRD

Observation of morphological behavior with heating of volcanic ash by in situ particle image analysis

HAMADA, Hiroyuki^{1*} ; KANATSUKI, Shinichiro² ; HAYAUCHI, Aiko¹ ; SASAKURA, Daisuke¹

¹Malvern Instruments, A division of Spectris Co., Ltd., ²Japan High Tech Co., Ltd.

1. Introduction

An *in-situ* observation to particle morphology under any perturbations is well used to understand physical chemistry behavior of mineral particles. With using by a heating response as a one of perturbation is interesting to investigate to melting and crystallinity of minerals. One of drawback to particle morphology investigation by a manually microscope is a qualitative approach rather than quantitative approach.

Our group has reported particle characterization and classification of a volcanic ash fine particle using by images for the purpose of determining particle size distribution which is based on described in ISO13322. The particles are appropriately dispersed and fixed on an optical microscope implemented an automated real time particle image analysis function on software. This report will be discussed for observation of morphological behavior with heating of volcanic ash by in situ particle image analysis.

2. Material and Method

In this study, the volcanic ash was sampling from Ito flow in Kagoshima. As a statistical particle image analysis, an automated particle image analyzer, Morphologi G3-SE (Malvern Instruments) was used for evaluation of particle size and shape. The observation mode was reflectance mode magnification was 75x in total magnification. The sample was dispersed with SDU (Sample Dispersion Unit) which attached Morphologi G3-SE. Number of measured particles was several hundred and a parameter filter function on software was used based on shape and pixel number of particle image. As a heat stage, Linkam stage TS1500 (Japan Hightech Co., Ltd.) was use for sample heating up to 1500 °C. A sample particle was dispersed on a platinum sample cell by SDU.

3. Result and Discussion

As a result of feasibility study, Fig.1 shows the observed images at 30 °C, 500 °C, 1000 °C, and 1500 °C. No change was observed between 30 °C and 1000 °C. However, the significant change of particle morphology by melting was observed between 1000 °C and 1500 °C. Refer to result of feasibility test, the temperature range from 1000 °C to 1500 °C is appropriate for this investigation.

4. Conclusion

In summarize of this study, it was possible to observe particle morphology change by heating. This report will be more discussed about the application and the capability for more quantitative investigation by particle image analysis.

Keywords: volcanic ash, microscopy, particle image analysis, particle diameter, particle distribution

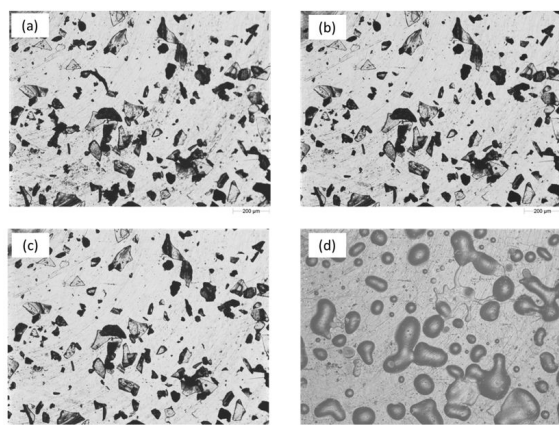


Fig.1 Particle morphology change under heating. (a)30°C (b)500°C (c)1000°C (d)1500°C

Magnetic measurement of H₂O at low-temperature and high-pressure

KONDO, Tadashi^{1*} ; KAKEDA, Takafumi¹ ; TANIGUCHI, Toshifumi¹

¹Graduate School of Science, Osaka University

Water ice is universal material in space and has fifteen polymorphs reported so far. Because of difficulty in detection of subtle structure change corresponding to hydrogen shift, and slow kinetics of low-temperature ice, some phase boundaries at low temperature are still not confirmed experimentally, which is very important information in planetary science. In this study, we tested a possibility of new method for studying structural change of ice using magnetic measurement at low-temperature and high-pressure. H₂O is diamagnetic substance, and the signal intensity of magnetic susceptibility is not detectable if we use a conventional method of magnetic measurement. However, positional ordering of hydrogen atoms should change the spin state of ice. Therefore, we can expect finite change in magnetic susceptibility.

Magnetic measurements were conducted in Superconducting Quantum Interference Device magnetometer (SQUID, MPMS-7, Quantum design). We measured the magnetic moment of ice at temperature below room condition. The measurement was also conducted at high-pressure condition to 0.2GPa to detect phase boundary between phase IX and phase I. Highly purified water with 5 M ohm resistivity or salted waters was used as starting sample in the Teflon capsule with /without a piston cylinder type high pressure cell made of beryllium copper alloy. After many trials of accurate evaluation of magnetic moment of all material surrounding sample as background signal to be subtracted, we measure the signal with water ice in the capsule. The magnetic field applied was 1T. The sample was first cooled to around 100K, then, the temperature elevated to room condition at the rate of 0.25K/s.

Solid-liquid transition of pure water was reproducibly detected with abrupt decrease of magnetic susceptibility. In the case of salt water, magnetic susceptibility decreased gradually with a temperature width as figured by thermodynamics. In the high-pressure run, we found an another jump in the profile of magnetic susceptibility measurement. The condition was close to solid-solid phase boundary proposed. We will report further detail of the experiments as possible detection of phase change in low-temperature water ice.

Keywords: water ice, magnetic measurement, high pressure, phase transition, SQUID